

Intravoxel incoherent motion diffusion-weighted MR imaging of gliomas: feasibility of the method and initial results

Sotirios Bisdas · Tong San Koh · Constantin Roder · Christian Braun · Jens Schittenhelm · Ulrike Ernemann · Uwe Klose

Received: 22 March 2013 / Accepted: 26 June 2013 / Published online: 14 July 2013
© Springer-Verlag Berlin Heidelberg 2013

Abstract

Introduction The purpose of this study was to evaluate the feasibility of intravoxel incoherent motion (IVIM) imaging and its value in differentiating the histologic grade among human gliomas.

Methods The IVIM model generated parametric images for apparent diffusion coefficient ADC, slow diffusion coefficient D (or D_{slow}), fast diffusion coefficient D^* (or D_{fast}), and fractional perfusion-related volume f in 22 patients with gliomas (WHO grade II–IV) using monopolar Stejskal–Tanner diffusion-weighted imaging (DWI) scheme and 14 b values ranging from 0 s/mm² to a maximum of 1,300 s/mm². A region-of-interest analysis on the tumor as well as in the white matter was conducted. The parameter values were tested for significant differences. The repeatability of the measurements was tested by coefficient of variation and Bland–Altman plots. **Results** D , D^* , and f in the high-grade gliomas demonstrated significant differences compared to the healthy white matter. D^* and f showed a significant difference between low- and

high-grade gliomas. D tended to be slightly lower in the WHO grade II compared to WHO grade III–IV tumors. f and D^* demonstrated higher coefficients of variation than the ADC and D in tumor. The Bland–Altman plots demonstrated satisfactory results without any outliers outside the mean±1.96 standard deviation.

Conclusion The IVIM-fitted post-processing of DWI-signal decay in human gliomas could show significantly different values of fractional perfusion-related volume and fast diffusion coefficient between low- and high-grade tumors, which might enable a noninvasive WHO grading in vivo.

Keywords Gliomas · Diffusion-weighted imaging · Perfusion

Introduction

In 1988, Le Bihan et al. [1] defined intravoxel incoherent motion (IVIM) as the microscopic translational motions that occur in each image voxel during an MRI acquisition. In biological tissues, these motions include molecular diffusion of water and microcirculation of blood in the capillary network. Microcirculation of the blood in capillary network (perfusion) can also be considered as an incoherent motion since the capillary organization can be seen at the voxel size as random [1]. These two phenomena account for the bi-exponential decay of the signal observed on diffusion-weighted imaging (DWI) when different diffusion b values are applied. The IVIM modeling allows the extraction of two diffusion coefficients, one related to molecular diffusion restriction, D (also known as D_{slow}), another related to the tissue perfusion called D^* (also known as D_{fast}), and finally the vascular volume fraction f . The contribution from larger (feeding or draining) vessels, in which blood velocity is higher, is more or less spoiled by the presence of the magnetic-pulsed gradients [1].

Besides the pioneer work of Le Bihan et al. [1], the use of IVIM modeling of DW-MRI data in human gliomas has not

S. Bisdas (✉) · U. Ernemann · U. Klose
Department of Diagnostic and Interventional Neuroradiology,
Eberhard Karls University, Hoppe Seyler Str. 3, 72076
Tübingen, Germany
e-mail: sotirios.bisdas@med.uni-tuebingen.de

T. S. Koh
Department of Oncologic Imaging, National Cancer Center,
Singapore, Singapore

C. Roder
Department of Neurosurgery, Eberhard Karls University, Tübingen,
Germany

C. Braun
Department of Neurology, Eberhard Karls University, Tübingen,
Germany

J. Schittenhelm
Department of Neuropathology, Eberhard Karls University,
Tübingen, Germany

been reported. Furthermore, there is no evidence regarding the repeatability of the IVIM-modeled parameters measurements in the human gliomas. The applicability of IVIM modeling as a means of preoperative tumor grading may also be beneficial in the glioma imaging since the method is not associated with radiation burden or the external application of a paramagnetic contrast agent for estimation of perfusion-related parameters. Therefore, the purpose of our study was to verify the feasibility of acquisition of diffusion- and perfusion-sensitized images in a sample of low- and high-grade gliomas as well as to assess any differences concerning the IVIM-based parametric images (D , D^* , and f) between the two gliomas subgroups, which may enable a non-invasive grading in vivo.

Materials and methods

The local Institutional Review Board approved this prospective study, and a written informed consent was obtained from all participants. Siemens Medical Systems (Erlangen, Germany) endorsed technical support for the applied DWI sequence appropriate for IVIM estimations. The authors are not associated with Siemens Medical Systems and maintained full control of the data at all times.

Patients

Twenty-two consecutive patients (12 women, 10 men; average age, 65 years; age range, 37–75 years) were enrolled in this study and underwent DWI of brain tumors prior to any treatment. All of these patients were known to have gliomas from results of clinical examination and conventional magnetic resonance (MR) imaging, performed prior to this study. Exclusion criteria were general contraindications to MR imaging, such as implanted pacemaker and claustrophobia. The primary sites of the gliomas included the occipital lobe ($n=3$), the frontal lobe ($n=5$), temporal lobe ($n=8$), and the parietal lobe ($n=6$). In order to test the repeatability of the DW-MR images acquired for the IVIM modeling, eight randomly chosen patients (three with low-grade and five with high-grade gliomas) underwent after informed consent another DW-MR imaging exam 2 days after the initial imaging on the same MR scanner with no medical treatment administered in between.

Conventional MR imaging

MR imaging was performed by using a 1.5-T MR scanner (Magnetom Avanto; Siemens Medical Systems, Erlangen, Germany) with a 12-channel phased-array coil. After obtaining axial T2-weighted fluid attenuated inversion recovery (FLAIR) (repetition time (TR) in milliseconds/echo time (TE) in milliseconds, 9,000/103) MR images, T1-weighted images (TR/TE, 450/15 ms) were acquired before and after intravenous, body-

weight adapted administration of gadobutrol (Gadovist®, Bayer-Schering, Berlin, Germany), followed by a 20-ml saline flush.

DW-MR imaging

The sequence was based on standard single-shot DW spin-echo echo-planar imaging with the following parameters: TR/TE of 3,300/83 ms, GRAPPA accelerator factor of 2, field of view 230×230, base resolution of 128×128, 10 slices with thickness of 3 mm, intersection gap of 1.5 mm, number of averages 2, bandwidth of 751 Hz, and acquisition time of 3 min 40 s. Axial, three-scan-trace DW-images, prior to gadolinium administration, were acquired with multiple b values ranging from 0 s/mm² to a maximum of 1,300 s/mm² (0, 5, 10, 20, 30, 40, 60, 80, 90, 100, 200, 700, 1,000, 1,300). The used sequence scheme was a monopolar Stejskal–Tanner implementation. On the processing side, an image-based correction of eddy current induced distortions was enabled.

Post-processing of DW-MR imaging

In this study, exponential ADC images (including all b values) and extrapolated trace images could be generated. Subsequently, the IVIM algorithm described by the bi-exponential Eq. (1) below, running on vendor's software generated on-line D , D^* , and f images, where D and D^* are the diffusion parameter related with molecular diffusion and with the incoherent microcirculation, respectively, S is the mean signal intensity, and f is the perfusion fraction:

$$S/S_0 = (1-f) * \exp(-b * D) + f * \exp(-b * (D + D^*)) \quad (1)$$

Three different approaches may be applied to generate parametric images (D , D^* , and f): full bi-exponential fit, initial estimation of D using a reduced set of b values larger than a predetermined value and then using the resulting D as a fix parameter to fit the missing parameters [2], and D^* with a given value using it in the bi-exponential model to fit the missing values [3]. We found that the second approach delivered the most robust and signal-to-noise enhanced results in all cases, and thus, it was used for the subsequently performed metrics in all patients. b values higher than 200 s/mm² were used to estimate D .

The analysis of the voxel-wise calculated parametric maps was based on hand-drawn region-of-interest (ROI) that were manually placed by two neuroradiologists in consensus on the tumor area with the largest diameter encompassing as much of the solid tumor area as possible. We used T1-weighted contrast-enhanced images where blood–brain barrier disruption was present or FLAIR images in tumors without contrast agent leakage as references to determine tumor areas

on the corresponding DWI-derived IVIM images. A rigid co-registration between diffusion-weighted and anatomical images was not preferred. Visually cystic, hemorrhagic, or necrotic areas as well as cerebrospinal fluid (CSF)-filled spaces were excluded from the analysis. Before performing the ROI placement in consensus, the two readers assessed independently the tumors in the D , D^* , and f maps in all patients and the values were recorded in order to estimate the inter-rater variability. The mean ROI area was $130.1 \text{ mm}^2 \pm 56.6$ (range, $59.2\text{--}455.2 \text{ mm}^2$). For the contralateral healthy appearing white matter, standardized ROIs (size, 50 mm^2) were placed in the centrum semiovale without including leptomeningeal vessels and gray matter.

Statistical analysis

The extracted parameter values ADC, D , D^* , and f were tested for significant differences between tumor sites and contralateral healthy white matter by appropriately used parametric (Welch's t test) or non-parametric tests (Mann–Whitney U test) according to data normality (Kolmogorov–Smirnov test) (MedCalc Software, Mariakerke, Belgium). The repeatability of the IVIM results was tested by the calculation of the coefficient of variation and the Bland–Altman plots for the duplicate measurements. The data introduced in the Bland–Altman analysis showed either a normal distribution or were logarithmically transformed. The inter-rater agreement was assessed by the Kappa value. Kappa values between 0.61 and 0.80 indicate a good strength of agreement, while values >0.81 indicate a very good agreement between the raters. A significant value of P less than 0.05 was considered statistically significant.

Results

All DWI exams with multiple b values were suitable for post-processing, and the fitting process was successful. Figure 1 demonstrates the bi-exponential fitting of the diffusion signal decay in a case of high-grade glioma. All excised tumors were histologically diagnosed and included seven diffuse astrocytomas gliomas WHO grade II, six with astrocytomas WHO grade III, and nine astrocytomas WHO grade IV (glioblastomas—GBMs). WHO grade III and IV gliomas were included in the group of high-grade tumors for further analysis. Representative anatomic images as well as parametric maps in two patients with histologically verified gliomas WHO grades 2 and 4 are demonstrated in Fig. 2. Table 1 shows the descriptive statistics of the ADC and IVIM parameters (D , D^* , and f) in the low- and high-grade gliomas as well as in the contralateral healthy white matter. The values of all examined parameters except of the D^* values in the healthy white matter showed a normal distribution. The

relative standard deviations (SDs), which indicated the variance of the measured parameters, were lower in the healthy parenchyma than in the tumor sites ($P \leq 0.03$) and were not significantly different between the two histologic types of gliomas. D^* and f showed a significant difference between low- and high-grade gliomas with $P=0.001$ and $P=0.02$, respectively (Fig. 3), whereas D tended to be slightly lower in the WHO grade II compared to WHO grade III–IV tumors. Finally, the D , D^* , and f acquired in the high-grade gliomas demonstrated significant differences compared to the healthy white matter ($0.001 \leq P \leq 0.04$). A trend to statistical significance was also observed for the D ($P=0.055$) and ADC ($P=0.06$) between low-grade gliomas and healthy white matter.

The inter-rater agreement for the D , D^* , and f values was generally good. The Kappa values were 0.70 (95 % CI, 0.54–0.87), 0.67 (95 % CI, 0.47–0.87), and 0.83 (95 % CI, 0.78–0.88), respectively. Regarding the repeatability of the IVIM-based parameters, higher coefficients of variations were shown for f (16.1 %) and D^* (13.8 %) than for ADC (5.9 %) and D (7.5 %) in tumor tissue. In contrary, the coefficient of variation in the healthy white matter did not exceed 8 % for all parameters. The Bland–Altman plots demonstrated in all cases satisfactory results without any outliers outside the $\text{mean} \pm 1.96 \text{ SD}$ boundaries, which are considered to be clinically relevant. The second control MRI measurement provided in the majority of cases lower values than the first one, which resulted in a positive difference of the means as depicted in the y -axis of the Bland–Altman plots (Fig. 4). In Bland–Altman plots, ADC, D^* , and D in tumors showed a trend for an underestimation of the retest values proportional to their size (Fig. 4). However, this trend was partly artificial, as it seemed to be caused by individual measurements and accentuated by the small patient sample. Interestingly, the Bland–Altman plot of the f values in tumor tissue (Fig. 4) showed very satisfactory results, which were in contrast to the coefficient of variation that was found to be the highest among all other parameters.

Discussion

Diffusion-weighted signal decay in brain has been shown to be multi-exponential, and the bi-exponential model may be a better way to describe the admixture of multiple exponential signal decays [4]. However, the bi-exponential model is probably also an oversimplification of reality, and it is more realistic, according to Bennett et al. [5], to assume a larger number (>2) of intravoxel proton pools with different diffusion coefficients [6]. Federau et al. recently demonstrated the sensitivity of IVIM-based measurements of brain perfusion in subjects under hypercapnia-induced vasodilatation and hyperoxygenation-induced vasoconstriction [7]. They also

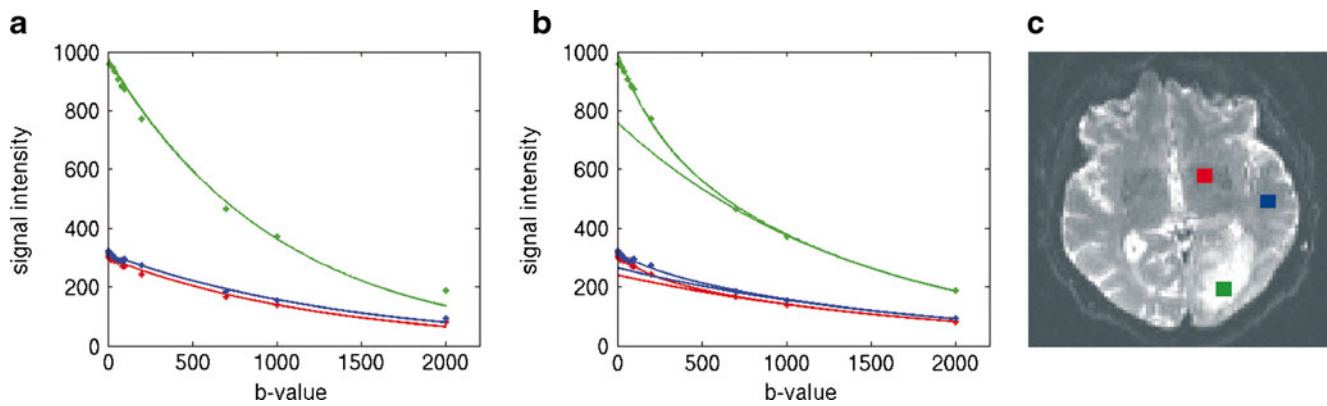


Fig. 1 Mono- (a) and bi-exponential (b) fitting of the diffusion signal decay over a wide-range of b values (up to 2,000, though the highest one was not used for the analysis due to the known SNR shortcomings at these b values level) in a patient with glioblastoma on the left temporal–occipital region (c). Regions of interest were seeded in the

tumor tissue (*green*), white matter (*blue*), and basal ganglia (*red*). The mono-exponential fitting line clearly shows that the signal decay cannot be adequately described. In contrary, the bi-exponential method provides a satisfactory result (the interception of the fitting line obtained by high b values with the y -axis is also shown)

showed that the variance for the ROIs measurements was higher than for the whole-brain results; this finding is in concordance with the high SDs that were also demonstrated in our study. This variance may be explained by an intrinsic inhomogeneity regarding diffusion- and perfusion-related values in gliomas as well as by a physiologic variability in

normal tissue. The higher variance in fast diffusion parameters than in the slow diffusion values may also reflect the variably increased capillary perfusion across tumors, especially the high-grade gliomas [8].

Interestingly, the D^* estimates did not significantly differ between normal tissue and low-grade gliomas, while f values

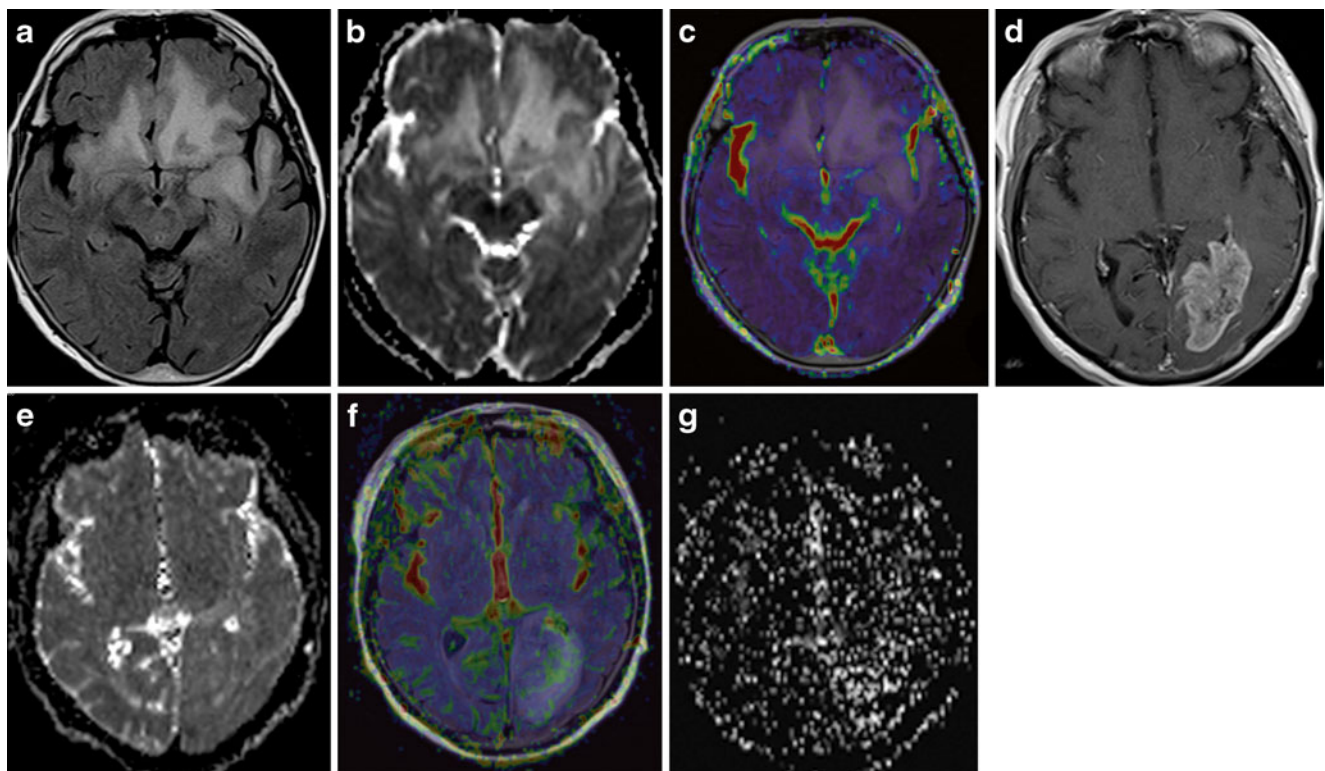


Fig. 2 The axial FLAIR image (a) shows a hyperintense mass on the left temporal lobe crossing the midline without any gadolinium enhancement (image not shown) in a patient with grade II glioma. The D map (b) demonstrates an inhomogeneous intrinsic hyperintensity in the tumor while the f map (c), encoded in a blue–green–red (in increasing value order) color schema, shows no regions with increased perfusion fraction compared to the healthy parenchyma. The gadolinium-

enhanced T1-weighted image in a patient with a glioblastoma shows the tumor mass located in the left occipital lobe (d). The D map (e) fails to delineate the tumor, whereas the f map (f) demonstrates the gadolinium-enhancing region of the tumor as foci with higher perfusion fraction compared to the healthy white matter. The D^* map (g) demonstrates the increased fast-diffusion values in the tumor tissue on the left occipital lobe

Table 1 Descriptive statistics of the IVIM-derived parameters in the tumor sites separated by their histological grade in low- and high-grade gliomas as well as in the healthy white matter

	LGG	HGG	WM	P-value (LGG vs. HGG)
ADC	0.71±0.12	0.76±0.15	0.65±0.05	0.09
D^*	10.8±7.8	41.6±26.1	7.3±6.1	0.001
D	0.52±0.28	0.76±0.49	0.62±0.21	0.07
f	6.1±3.9	10.7±8.3	6.5±3.7	0.02

The P values of the comparison of the parameters between low- and high-grade gliomas are also given (the significant ones are indicated in bold italics). ADC, D , and D^* in 10^{-3} mm²/s, f in percent

LGG low-grade gliomas (WHO grade II), HGG high-grade gliomas (WHO grade III-IV), WM white matter

proved to be slightly higher in healthy white matter than in low-grade tumor. This may be attributed to the unavoidable contamination effect due to inclusion of microscopical capillaries and CSF spaces in the ROI analysis of white matter. Thus, the choice of the ROI is of crucial importance, whereas the susceptibility of D^* values in this and other acquisition-related issues (analyzed in the following) is also reflected in the non-normal distribution of D^* values in the healthy white matter. Nonetheless, this variance may also be the result of an impaired quality of the IVIM maps [9]. There are several reasons that contribute to moderate quality of the f , D , and D^* maps. Firstly, the IVIM effect in the brain, where the reported perfusion fraction f is reported to be low [10], is rather restricted compared to abdominal organs like liver and kidneys. Secondly, the available signal-to-noise ratio (SNR) may be below the critical value and the calculation of the IVIM parameters in a reliable fashion to be impossible. Systematic errors such as patient movement or partial volume

effects may also hamper the quality of the maps. Finally, the inadequate choice of the applied b values may have a detrimental effect on the acquired IVIM maps and low SNR implies the need for more b values in order to obtain reliable results. Thus, it is proposed to acquire 30 or more b values for the optimal assessment of the IVIM parameters [9]. However, in the vast majority of the cases, the acquisition of 30 or more b values is not acceptable due to scan time restrictions. Lemke et al. suggest that at least 10 of the optimally distributed b values reported in their work should be measured for a high-quality IVIM experiment [9], and our present study was conducted accordingly. Finally, the aforementioned variances might not be relevant when estimation of the average f , D^* , D , and ADC values results from large-sized tumor ROIs. This technique is more robust compared to pixel-to-pixel analysis [9, 11] or estimations of maximal values, which in case of inadequate SNR may be artificial.

Compared to abdominal imaging, the IVIM-modeled DWI in brain has some inherent difficulties. CSF may flow similar to blood, and thus, the diffusion coefficient will be higher than that of water in vitro. It is also postulated that the co-existence of several velocities in a single CSF voxel may lead to non-uniform flow [2]. Le Bihan et al. [12] have suggested the use of flow-compensated bipolar gradient pulses for eliminating the effect of constant linear flow. In this direction, the implementation of an inversion recovery pulse in the applied DWI in order to eliminate the CSF signal may be also a robust solution to this problem. However, we think that such an inversion recovery pulse would not only minimize the CSF contamination effect but would also alter the relaxation curves of the normal parenchyma. Alternatively, the segmentation and subsequently extraction of the CSF-filled spaces from the calculations using the DWI source images may also improve the estimation of IVIM-based parameters.

Concerning tumor tissue, Pang et al. have reported that D estimations in prostatic tissue are capable of discriminating tumor from normal tissue due to their significant reduction [13]. Published works [14, 15] using 0 and 1,000 s/mm² b values for ADC estimations argued that it is possible to use ADC as a non-invasive means for glioma grading. However, the IVIM-derived ADC and D values failed to serve as surrogate markers for gliomas grading in the present work. The reason for this discrepancy might be the small patient cohort in our study (considering the trend to statistical significance for the D) as well as that the previous works took into account perfusion components by including $b=0$ s/mm². The contamination with perfusion-related phenomena may also explain why “lumped” ADC values were higher in high-grade compared to low-grade gliomas. Bi-exponential fitting provides tremendous advantage over ADC measures, which are dependent on the b value used for diffusion imaging [16, 17]. Alternatively, this result may imply that more than tumor

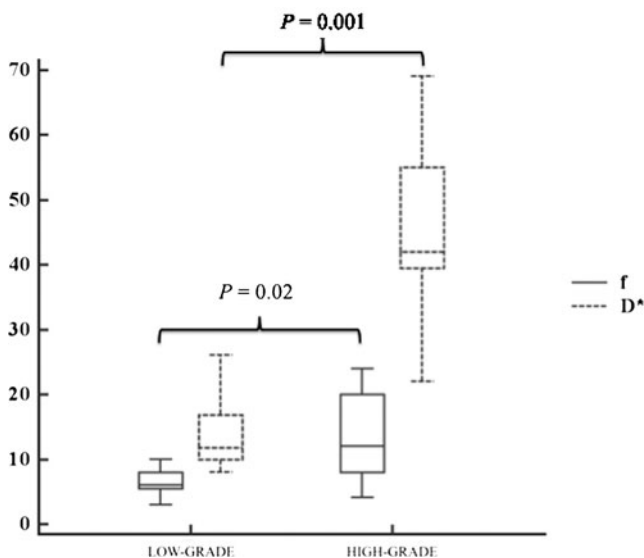


Fig. 3 Box-whisker plots for the D^* and f values in low- and high-grade gliomas. The statistically significant differences of the perfusion-related parameters between the histologic grades are also annotated

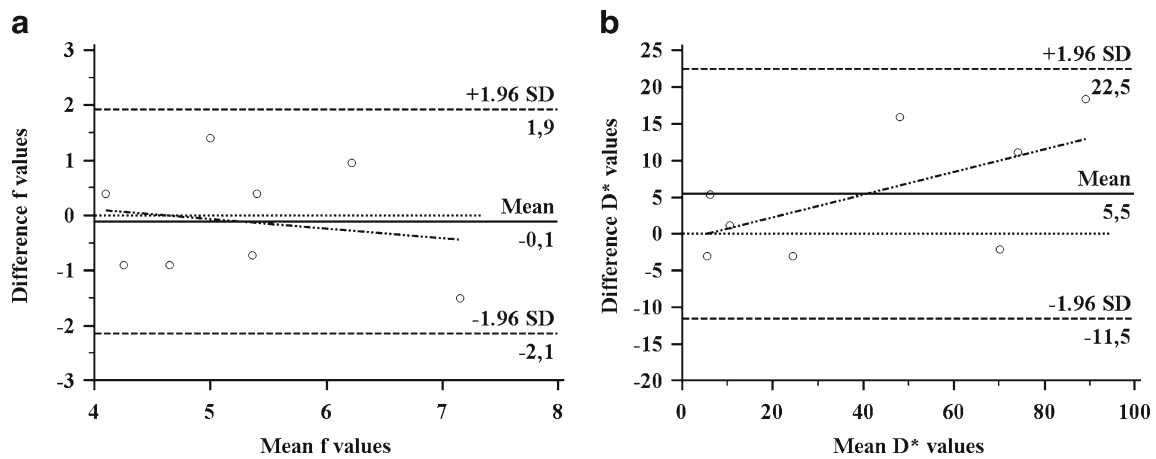


Fig. 4 Bland–Altman plots comparing the duplicate measurements in order to estimate the repeatability of the f (**a**) and D^* (**b**) values in tumor. The differences in the f and D^* values between the first and the second measurements (y -axis) are plotted against the averages of them (x -axis). The line of equality (*dotted line* at 0 in the y -axis) implies a perfect

cellularity the capillary neo-angiogenesis is contributing to the diagnostic ability of the IVIM model. Another interesting finding in this study was that a tendency to higher D values was observed in high-grade gliomas than in low-grade ones. This finding may reinforce the initial evidence that malignancy grade strongly corresponds to an increase in extracellular space volume, which is accompanied by alteration of the barriers for water molecules [18].

The reported values of IVIM-based perfusion-related estimates in the healthy white matter in this study are in essential agreement with the ones reported by Federau et al. in the normal brain parenchyma [7]. Interestingly, D^* proved to be significantly different between low- and high-grade gliomas providing a potential biomarker for future validation. Compared to the D^* maps, the f maps showed a better visual quality, appeared less noisy, and showed to be more homogeneous compared to previously published ones [20], which has to be attributed to the better gradient hardware and the echo planar imaging in high-field systems as well as to the lower coefficient of variation of f compared to D^* maps [21]. Measurements in healthy volunteers quantified the perfusion fraction f up to 4.5 % (full bi-exponential fit) and 6.7 % (asymptotic fitting), which is closer to our study [20]. These data are contradictory to the more recent data of the same group [19], which imply an overestimation of f calculated by full fitting procedures and probably reflect an uncertainty in the IVIM calculations depending on SNR and the fitting procedures. Similar to D^* values, f in our study was higher in high-grade gliomas compared to the low-grade tumors. This was a perspicuous finding, as f mainly reflects the vascular compartment and an increased cerebral blood volume (CBV) is known in glioblastoma compared to low-grade glioma. This finding may be useful for differentiating gliomas in future studies.

agreement, whereas the *solid line* indicates the mean difference between the two measurements. The *dashed regression line* of differences detects no substantial proportional difference (according to the size of the measured values). There are no outliers regarding the ± 1.96 SD borders

The potential clinical utility of IVIM-based perfusion-related estimates deserves more attention in the future. According to Wirestam et al. [19, 20], who found a modest but significant correlation between the perfusion fraction f and CBV measured by dynamic susceptibility-weighted contrast-enhanced MRI, f estimations may be surrogate parameters to the contrast-enhanced measurements of CBV. The quantification of cerebral perfusion, including also blood flow measurements, with contrast-enhanced dynamic imaging has also inherent shortcomings and is based on numerous assumptions that give an approximation of the real brain perfusion [22]. Similarly, arterial spin labeling, which like IVIM is based on intrinsic features of the brain tissue, has certain limitations [23]. Nevertheless, both methods possess evidence-based value in gliomas grading and would be interesting whether IVIM measurements may challenge or improve it [24]. Objections concerning the ability of IVIM technique to measure the classical “perfusion” as defined by the conventional tracer MR studies are raised, i.e., by Henkelman who believes that IVIM measures the flow in the direction of velocity encoding gradient, whereas classical perfusion measures the pattern of delivery [25, 26]. However, it seems that these two entities are distinct and have different units.

The inter-rater agreement was good for the D and D^* values, whereas the D^* values had slightly worse performance presumably due to their high sensitivity to capillary blood flow and any partial volume effect with CSF-filled or necrotic spaces. Interestingly, f maps demonstrated a very good strength of agreement, which justifies their utilization in future studies. In total, the repeatability was satisfactory without any outliers outside the $\text{mean} \pm 1.96$ SD, which is considered to represent the outer boundaries of clinically accepted repeatability. The results from the IVIM repeatability

analysis in this work are the first in brain tumors and are in essential agreement with the test–retest variability reported for f values in brain after ischemic injury as well as in healthy hemispheres, though in the latter study no similar metrics between the two experiments were provided [20]. The better repeatability of the IVIM parameters in the white matter compared to the tumor tissue was rather expected since the tumor tissue presents high fluctuations in the capillary bed microcirculation and D^* as well as f parameters have inherently higher coefficients of variation, reported not only in this glioma study but also in the literature data [27]. Moteki and Horikoshi assessing the reproducibility of IVIM measurements showed large variability of D and D^* values in liver cirrhosis with CoV of 25.4 and 28.2 % for D and D^* values; however, their study was with a limited number of b values, and they did not report CoV of ADC and f [25, 26]. f values in gliomas, which was shown to differentiate low- from high-grade gliomas, were adequately reproduced though their coefficients of variation were high. Nevertheless, the diagnostic confidence cannot be solely relied on IVIM imaging, but the latter acts mainly in a complementary way. What actually remains to be elucidated is whether the estimation of IVIM metrics and especially of f might be more appropriate for follow-up imaging and therapy monitoring in brain tumors.

Conclusion

IVIM-based DWI analysis provides parameters with a high potential for non-invasive, in-vivo grading of human gliomas by revealing the fast diffusion process of water molecules that takes place within tumor compartments under high-flow circumstances as well as the slow diffusion compartment of the tumor tissue. In our study, IVIM fitting of the diffusion data allowed separation of perfusion contribution from the true diffusion and thus provided greater insight compared to ADC in discriminating low- and high-grade gliomas. The significantly increased perfusion-related blood velocity, in terms of D^* and f , in high-grade compared to low-grade gliomas is consistent with the pathophysiology of the disease and offers another means, besides contrast-enhanced cross-sectional imaging and positron-emission tomography, for glioma staging. In this study, diffusion-related coefficient D did not facilitate any differentiation of gliomas grade but demonstrated a very satisfactory repeatability. At this point of time, modest visualization of the perfusion-related tissue properties is a certain drawback, which can be addressed by future studies before introduction of the technique into the clinical routine.

Conflict of interest We declare that we have no conflict of interest.

References

1. Le Bihan D, Breton E, Lallemand D et al (1988) Separation of diffusion and perfusion in intravoxel incoherent motion MR imaging. *Radiology* 168:497–505
2. Luciani A, Vignaud A, Cavet M et al (2008) Liver cirrhosis: intravoxel incoherent motion MR imaging—pilot study. *Radiology* 249:891–899
3. Lemke A, Laun FB, Klauss M et al (2009) Differentiation of pancreas carcinoma from healthy pancreatic tissue using multiple b -values: comparison of apparent diffusion coefficient and intravoxel incoherent motion derived parameters. *Invest Radiol* 44:769–775
4. Maier SE, Bogner P, Bajzik G et al (2001) Normal brain and brain tumor: multicomponent apparent diffusion coefficient line scan imaging. *Radiology* 219:842–849
5. Bennett KM, Schmainda KM, Bennett RT et al (2003) Characterization of continuously distributed cortical water diffusion rates with a stretched-exponential model. *Magn Reson Med* 50:727–734
6. Lee JH, Springer CS Jr (2003) Effects of equilibrium exchange on diffusion-weighted NMR signals: the diffusigraphic "shutter-speed". *Magn Reson Med* 49:450–458
7. Federau C, Maeder P, O'Brien K et al (2012) Quantitative measurement of brain perfusion with intravoxel incoherent motion MR imaging. *Radiology* 265:874–881
8. Bennett KM, Hyde JS, Schmainda KM (2006) Water diffusion heterogeneity index in the human brain is insensitive to the orientation of applied magnetic field gradients. *Magn Reson Med* 56:235–239
9. Lemke A, Stieltjes B, Schad LR et al (2011) Toward an optimal distribution of b values for intravoxel incoherent motion imaging. *Magn Reson Imaging* 29:766–776
10. Leenders KL, Perani D, Lammertsma AA et al (1990) Cerebral blood flow, blood volume and oxygen utilization. Normal values and effect of age. *Brain: J Neurol* 113(Pt 1):27–47
11. Pekar J, Moonen CT, van Zijl PC (1992) On the precision of diffusion/perfusion imaging by gradient sensitization. *Magn Reson Med* 23:122–129
12. Le Bihan D, Breton E, Lallemand D et al (1986) MR imaging of intravoxel incoherent motions: application to diffusion and perfusion in neurologic disorders. *Radiology* 161:401–407
13. Pang Y, Turkbey B, Bernardo M, et al. (2012) Intravoxel incoherent motion MR imaging for prostate cancer: an evaluation of perfusion fraction and diffusion coefficient derived from different b -value combinations. *Magnetic Resonance in Medicine: Official Journal of the Society of Magnetic Resonance in Medicine/Society of Magnetic Resonance in Medicine*. doi:10.1002/mrm.24277
14. Higano S, Yun X, Kumabe T et al (2006) Malignant astrocytic tumors: clinical importance of apparent diffusion coefficient in prediction of grade and prognosis. *Radiology* 241:839–846
15. Sadeghi N, Camby I, Goldman S et al (2003) Effect of hydrophilic components of the extracellular matrix on quantifiable diffusion-weighted imaging of human gliomas: preliminary results of correlating apparent diffusion coefficient values and hyaluronan expression level. *AJR Am J Roentgenol* 181:235–241
16. Braithwaite AC, Dale BM, Boll DT et al (2009) Short- and midterm reproducibility of apparent diffusion coefficient measurements at 3.0-T diffusion-weighted imaging of the abdomen. *Radiology* 250:459–465
17. Sigmund EE, Vivier PH, Sui D et al (2012) Intravoxel incoherent motion and diffusion-tensor imaging in renal tissue under hydration and furosemide flow challenges. *Radiology* 263:758–769
18. Vargova L, Homola A, Zamecnik J et al (2003) Diffusion parameters of the extracellular space in human gliomas. *Glia* 42:77–88
19. Wirestam R, Borg M, Brockstedt S et al (2001) Perfusion-related parameters in intravoxel incoherent motion MR imaging compared with CBV and CBF measured by dynamic susceptibility-contrast MR technique. *Acta radiologica* 42:123–128

20. Wirestam R, Brockstedt S, Lindgren A et al (1997) The perfusion fraction in volunteers and in patients with ischaemic stroke. *Acta Radiol* 38:961–964
21. Muller MF, Prasad PV, Edelman RR (1998) Can the IVIM model be used for renal perfusion imaging? *Eur J Radiol* 26:297–303
22. Knutsson L, Ståhlberg F, Wirestam R (2010) Absolute quantification of perfusion using dynamic susceptibility contrast MRI: pitfalls and possibilities. *MAGMA* 23:1–21
23. Petersen ET, Zimine I, Ho YC et al (2006) Non-invasive measurement of perfusion: a critical review of arterial spin labelling techniques. *Br J Radiol* 79:688–701
24. Bisdas S (2013) Are we ready to image the incoherent molecular motion in our minds? *Neuroradiology* 55:537–540
25. Henkelman RM (1990) Does IVIM measure classical perfusion? *Magn Reson Med* 16:470–475
26. Le Bihan D, Turner R (1992) The capillary network: a link between IVIM and classical perfusion. *Magn Reson Med* 27:171–178
27. Moteki T, Horikoshi H (2006) Evaluation of hepatic lesions and hepatic parenchyma using diffusion-weighted echo-planar MR with three values of gradient b-factor. *J Magn Reson Imaging* 24:637–645